A COARSE MESH RADIATION TRANSPORT METHOD FOR PRISMATIC BLOCK THERMAL REACTORS IN TWO DIMENSIONS

A Thesis
Presented to
The Academic Faculty

By

Kevin John Connolly

In Partial Fulfillment
Of the Requirements for the Degree
Master of Science in Nuclear Engineering

George W. Woodruff School of Mechanical Engineering
Georgia Institute of Technology

August 2011

A COARSE MESH RADIATION TRANSPORT METHOD FOR PRISMATIC BLOCK THERMAL REACTORS IN TWO DIMENSIONS

Approved by:

Dr. Farzad Rahnema, Advisor
George W. Woodruff School
Georgia Institute of Technology

Dr. Bojan Petrovic
George W. Woodruff School
Georgia Institute of Technology

Dr. Dingkang Zhang
George W. Woodruff School
Georgia Institute of Technology

Date Approved: June 17, 2011

ACKNOWLEDGEMENTS

I would like to express my appreciation for my advisor Dr. Farzad Rahnema for his guidance and confidence, Dr. Dingkang Zhang for his helpful suggestions that sent me in the right direction, and Dr. Bojan Petrovic for serving on my committee.

I would like to thank my family and friends for their support and encouragement throughout my time at Georgia Tech, especially my parents Kim and John Connolly and my wife Denise.

Lastly, I would like to acknowledge that this work was supported under a Nuclear Regulatory Commission (NRC) Fellowship, the Georgia Tech President's Fellowship, and a Department of Energy Nuclear Energy University Program (NEUP) Graduate Fellowship.

TABLE OF CONTENTS

LIST OF TABLES

LIST OF FIGURES

SUMMARY

In this paper, the coarse mesh transport method is extended to hexagonal geometry. This stochastic-deterministic hybrid transport method calculates the eigenvalue and explicit pin fission density profile of hexagonal reactor cores. It models the exact detail within complex heterogeneous cores without homogenizing regions or materials, and neither block-level nor core-level asymmetry poses any limitations to the method. It solves eigenvalue problems by first splitting the core into a set of coarse meshes, and then using Monte Carlo methods to create a library of response expansion coefficients, found by expanding the angular current in phase-space distribution using a set of polynomials orthogonal on the angular half-space defined by mesh boundaries. The coarse meshes are coupled by the angular current at their interfaces. A deterministic sweeping procedure is then used to iteratively construct the solution.

The method is evaluated using benchmark problems based on a gas-cooled, graphite-moderated high temperature reactor. The method quickly solves problems to any level of detail desired by the user. In this paper, it is used to explicitly calculate the fission density of individual fuel pins and determine the reactivity worth of individual control rods. In every case, results for the core multiplication factor and pin fission density distribution are found within several minutes. Results are highly accurate when compared to direct Monte Carlo reference solutions; errors in the eigenvalue calculations are on the order of 0.02%, and errors in the pin fission density average less than 0.1%.

1. INTRODUCTION

Several new reactor concepts, including the Next Generation Nuclear Plant (NGNP), are designed to be built with prismatic block cores. That is, their fuel assemblies are arranged in a hexagonal lattice. A representative example is the Very High Temperature Reactor (VHTR) (Idaho National Laboratory 2010), a graphite-moderated reactor which features strong heterogeneity at both the core and block level. This reactor is optically thin when compared to current water-moderated reactors, and the neutron angular flux exhibits stronger anisotropy than that in LWRs. Asymmetric blocks and the presence of burnable absorbers near fuel rods challenge low-order transport approximations (Lee et al. 2007), especially those which homogenize block structure. It is essential that robust reactor analysis methods exist which are capable of treating these new reactors. Therefore, a method which does not rely on homogenization and low-order approximations to the transport equation is desirable. The heterogeneous coarse-mesh transport (COMET) method (Mosher and Rahnema, 2006; Forget and Rahnema 2006b) has been shown to accurately determine the eigenvalue and power profiles of modern light water and heavy water reactors. This method does not homogenize regions, it does not resort to diffusion approximations, and it reaches solutions orders of magnitude faster than traditional Monte Carlo and fine mesh methods. However, it has only been demonstrated in water-moderated reactors on a Cartesian grid.

This study extends the COMET method into hexagonal geometry. In chapter 2, the COMET method will be briefly described. The extension of the method to hexagonal

geometry is discussed and implemented in chapter 3. The accuracy and efficiency of the method are evaluated in chapter 4; this chapter also includes a demonstration of the versatility of the method in calculating local effects, such as the worth of individual control rods, in highly heterogeneous and asymmetric environments. Concluding remarks and a discussion of future work are given in chapter 5.

2. BACKGROUND

The behavior of neutrons within a nuclear reactor core is described by the neutron transport equation (Bell and Glasstone, 1970):

$$\hat{\Omega}\cdot\nabla\psi\left(\vec{r},\hat{\Omega},E\right)+\sigma_t\left(\vec{r},E\right)\psi\left(\vec{r},\hat{\Omega},E\right)= \tag{1}$$

$$\int_0^\infty dE'\int_{4\pi} d\hat{\Omega}'\,\sigma_s\left(\vec{r},\hat{\Omega}',E'\rightarrow\hat{\Omega},E\right)\psi\left(\vec{r},\hat{\Omega}',E'\right)$$

$$+\frac{1}{4\pi}\chi\left(\vec{r},E\right)\int_0^\infty dE'\int_{4\pi} d\hat{\Omega}'\,\frac{\nu\sigma_f\left(\vec{r},E'\right)}{k}\psi\left(\vec{r},\hat{\Omega}',E'\right)+Q\left(\vec{r},\hat{\Omega},E\right)$$

It has as a boundary condition equation 2:

$$\psi\left(\vec{r}_b,\hat{\Omega},E\right)=B\,\psi\left(\vec{r}_b,\hat{\Omega}',E'\right),\quad \hat{n}\cdot\hat{\Omega}<0\quad and\quad \hat{n}\cdot\hat{\Omega}'>0 \tag{2}$$

The angular flux of neutrons is symbolized by ψ, and neutrons are defined within the volume to be at some position $\vec{r}$, traveling in some direction $\hat{\Omega}$, and to have some energy E. Macroscopic reaction cross-sections are denoted by σ, with t, s, and f specifying the types of reactions as total, scattering, and fission. In each fission, ν neutrons are introduced to the system within the energy spectrum χ. An external source Q may or may not be present; when it is absent, k represents the multiplication factor of the system. In the boundary condition given by equation 2, B is an arbitrary boundary

operator acting at a point $\vec{r}_b$ along the boundary of the core which has outward normal vector $\hat{n}$.

2.1. Reactor Analysis in Hexagonal Cores

Traditionally, reactor analysis methods have approximated equation 1 by using nodal diffusion techniques to quickly calculate eigenvalues and determine power profiles. Hexagonal lattice structure in cores challenges methods, as a coordinate system for two dimensional hexagonal geometry is not apparent. Some strategies, such as splitting the hexagonal blocks into six triangular nodes, have been implemented with success. Cho and Kim (1998) utilized a high order polynomial expansion diffusion method for 2-D triangular nodes. When compared with a fine mesh diffusion benchmark (Chao and Shatilla, 1995), their method calculated the multiplication factor with 30 pcm and the assembly power levels to an average error of under 1% within seconds. More recently, González-Pintor et al. (2009) demonstrated a high order finite element diffusion method which also divided the hexagonal assemblies into triangular nodes. Compared to the same fine mesh diffusion benchmark as before, this method calculated the eigenvalue of the core to an error within 1 pcm in seconds, along with the assembly average powers to less than 0.25% error, with an average error of less than 0.1%. However, these results are for VVER-style reactor cores and are in comparison to those obtained using the diffusion code DIF3D. When DIF3D has been compared to a Monte Carlo solution for a 2-D VHTR-style core (Lee et al. 2007), it requires the use of surface-dependent discontinuity factors to keep the error in the eigenvalue calculation below 300 pcm when control rods

are present in fuel blocks or below 650 pcm for cores with control rods present in reflector blocks. Even with these surface-dependent discontinuity factors, the average error in the block-averaged fission density are below 5%, but the maximum error approaches 13%, depending on the method for generating cross sections for the calculations. Without the use of surface-dependent discontinuity factors, eigenvalue calculations are in error by more than 1%, and the maximum error in the block-averaged fission density ranges from 12.9% to 18.9%. Control rod worth calculations have errors of up to 25%, although this is reduced to within 10% when surface-dependent discontinuity factors are used and in some cases was found to an error of as low as 1.9%.

Thilagam et al. (2009) have demonstrated a method to calculate the pin power levels individually throughout a hexagonal core by homogenizing individual pin cells and solving the entire core pin by pin. When compared to a Monte Carlo benchmark solution, this method has calculated the fission rate for pins in selected assemblies with no gadolinium present to errors of within 5%, and errors up to 7.3% for mixed uranium-gadolinium pins. Assembly-averaged fission rates were calculated within 8% of the benchmark, and the core multiplication factor was found to an error of within 200 pcm. The core benchmark used was an uncontrolled VVER-style light water reactor problem. However, when the benchmark problem was changed to a controlled VVER-style reactor, the error in the multiplication factor determined by this method increased to 1500 pcm, and the assembly-averaged fission rate had a maximum error of 15.7%. For a more accurate detailed solution, such as the fission density distribution for every pin in a core to an error of within 1%, or for calculations within heterogeneous reactors where control

blocks are present, it is clear that a method is necessary which does not rely on homogenization or diffusion techniques.

As computational resources have improved, methods based on solving the transport equation without approximation have gained in popularity. Methods such as fine mesh transport and stochastic methods are now more frequently used, as they offer greater accuracy than low-order approximations such as diffusion. Stochastic methods, such as MCNP (X-5 Monte Carlo Team, 2005) are able to treat complicated geometric specifications to a very high degree of accuracy, but the calculation of a precise detailed solution, such as the explicit pin power distribution, comes with a high computational price for large systems. The reference solutions used in chapter 4 of this paper were determined using stochastic methods, and required days of computing time.

Deterministic methods exist which are capable of treating thermal reactors with hexagonal geometry. Cho et al. (2007) demonstrated their use of the DeCART method with hexagonal capability in solving a 2-D eigenvalue problem based on the VHTR. When compared to a Monte Carlo reference solution, the eigenvalue error was found to be between 200 and 600 pcm, and block-averaged power levels were found to a maximum error of below 0.5%. Their solution of the full-core problem took approximately four hours of computing time. As this is an example of hexagonal functionality being added to an existing transport method for Cartesian geometry, let us consider other such methods.

A collection of results from various deterministic methods has been compiled for a benchmark based on a 2-D PWR problem (Smith et al., 2003). A variety of methods demonstrated their ability to solve the eigenvalue problem to an error of under 250 pcm as well as the pin power distribution to a mean relative error of under 1%. Most of these methods required days or hours of computing time to reach a solution, while a couple took only minutes. However, the COMET method solved the problem with an eigenvalue error of 120 pcm and a mean relative error in the pin power calculation of 0.56%, and required only seconds of computing time to reach the solution (Forget et al., 2004). As this method has been shown to be fast and highly accurate, this paper will extend its functionality in order to treat hexagonal geometry in full core problems.

2.2. A Hybrid Coarse Mesh Transport Method

The method developed in this paper is a hybrid with the robust geometric capability of a Monte Carlo method, but it takes advantage of a deterministic procedure in order to produce a solution at a greatly enhanced speed and with comparable accuracy. For the sake of clarity, a brief summary of the COMET method is presented here. COMET is an incident flux response expansion method (Mosher and Rahnema, 2006) which solves reactor core eigenvalue problems by dividing the reactor into a set of heterogeneous coarse meshes.

The method uses a set of pre-computed response functions to iteratively solve a full-core transport problem. The problem is divided into a series of smaller local problems without

approximation, by first splitting the core into a collection of non-overlapping coarse meshes which are coupled by the angular current at their interfaces. The transport equation within each mesh *i* becomes

$$\hat{\Omega}\cdot\nabla\psi_i\left(\vec{r},\hat{\Omega},E\right)+\sigma_t\left(\vec{r},E\right)\psi_i\left(\vec{r},\hat{\Omega},E\right)= \tag{3}$$

$$\int_0^\infty dE'\int_{4\pi} d\hat{\Omega}'\sigma_s\left(\vec{r},\hat{\Omega}',E'\rightarrow\hat{\Omega},E\right)\psi_i\left(\vec{r},\hat{\Omega}',E'\right)$$

$$+\frac{1}{4\pi}\chi\left(\vec{r},E\right)\int_0^\infty dE'\int_{4\pi} d\hat{\Omega}'\frac{\nu\sigma_f\left(\vec{r},E'\right)}{k}\psi_i\left(\vec{r},\hat{\Omega}',E'\right)+Q_i\left(\vec{r},\hat{\Omega},E\right)$$

with boundary condition

$$\psi_i\left(\vec{r}_{ij},\hat{\Omega}_i,E\right)=\psi_j\left(\vec{r}_{ij},\hat{\Omega}_j,E\right), \tag{4}$$

where mesh *i* and mesh *j* meet at the surface defined by $\vec{r}_{ij}$ and, where $\hat{n}_i$ designates the outward normal of mesh *i*, $\hat{n}_i\cdot\hat{\Omega}_i=-\hat{n}_j\cdot\hat{\Omega}_j$. Here the value *k* is the multiplication factor of the entire core; it is not an eigenvalue of equation 3. For a typical water-moderated reactor core calculation, each coarse mesh would be the size of a fuel assembly. Fixed-source calculations are conducted on each unique coarse mesh in order to determine the outgoing angular current as a response to a given incoming angular current. A unique coarse mesh depends only on the mesh geometry and material composition. Forget and Rahnema (2006b) use a Monte Carlo method to conduct these

calculations, as it allows the material and geometry specifications of the mesh to be modeled exactly without approximation.

The COMET method generates response functions using the fact that any angular partial current distribution over a face *f* of a mesh *i* can be given as the sum of a complete set of functions $\Gamma^a(\vec{w})$ orthogonal over the half-space $\vec{w}$ defined by a coarse mesh face, as shown in equation 5.

$$J_{if}^{\pm}(\vec{w}) = \sum_{a=0}^{\infty} c_{if}^{a} \Gamma^{a}(\vec{w}) \tag{5}$$

For the method to be practical, the series is truncated at an order high enough to preserve accuracy. In order to generate a library of response functions, a fixed-source calculation is conducted at all desired expansion orders *a* using an incoming angular current source on face *f* of mesh *i* equal to the distribution Γ^a. The outgoing angular current J^+ from each face *f'* is tallied in terms of the orthogonal function set chosen, and the coefficients *c*, found using equation 6, are stored in a database to be used for solving the full core problem.

$$c_{if'}^{a} = \int J_{if'}^{+}(\vec{w}) \Gamma_{if'}^{a}(\vec{w}) d\vec{w} \tag{6}$$

Response functions for the fission density within each pin in a mesh are also calculated and tabulated. In the interest of computational efficiency, response function calculations

are conducted by solving equation 3 using several different values of k. The solution procedure interpolates between the calculated response expansion coefficients to determine the coefficient for a desired core multiplication factor.

The solution to the full-core problem is composed iteratively using the response functions. A two-level iteration procedure is used to determine the core eigenvalue and the partial currents at mesh interfaces throughout the core. An initial guess is made for the eigenvalue and partial currents, and the guess is improved using a deterministic sweeping process. Starting at some mesh, the outgoing angular current from each face of that mesh is determined from the incoming angular current using linear superposition of the response functions. The outgoing current from one mesh becomes the updated guess for the incoming angular current for the neighboring mesh. Iterations are conducted until all calculated partial currents converge to a desired limit. Once convergence is reached for the inner iterations, the multiplication factor k is re-calculated using the neutron balance method. Outer iterations continue until convergence of the eigenvalue, at which point the fission density of each pin will be known, and the full-core problem has been solved.

3. METHOD

Recognizing that the existing coarse mesh transport method for water-moderated reactors in Cartesian geometry quickly produces accurate results (Forget and Rahnema, 2006a, 2006b, 2006c), it is used as the starting point for the hexagonal coarse mesh method. The following sections describe the extension to hexagonal geometry. The method consists of three steps. First, fixed-source calculations are conducted stochastically to determine the incident current response expansion coefficients necessary to solve the problem. Second, these solutions are compiled in a library. Finally, a deterministic solution method calculates the core eigenvalue and pin fission density distribution.

3.1. Response Coefficient Generation

Following in the method of Forget and Rahnema (2006b), a tensor product of shifted Legendre polynomials is chosen as the orthogonal set in which to expand the angular current:

$$\Gamma^a\left(\vec{r},\hat{\Omega},E\right)=\widetilde{P}_l^{[0,U]}(u)\widetilde{P}_m^{[-1,1]}(\mu)\widetilde{P}_n^{[0,\pi]}(\varphi)\delta_g \tag{7}$$

The reference system will be defined by the mesh face, where the spatial variable u extends along the length of the mesh face from 0 to U, the azimuthal angle φ from the mesh face is defined from 0 to π, and μ, the cosine of the polar angle from the mesh face, extends from -1 to 1. Figure 1 illustrates the relationship between the mesh coordinate

system and the Cartesian coordinate system. Using the multigroup treatment of the energy variable over *G* groups, the angular current on face *f* of mesh *i* becomes

$$J_{if}^{\pm}\left(\vec{r},\hat{\Omega},E\right)=\sum_{a=1}^{\infty}c_{if}^{a}\Gamma^{a}\left(\vec{r},\hat{\Omega},E\right) \quad . \tag{8}$$

Here an approximation to the transport equation is introduced by truncating the infinite sum of the orthogonal series.

A method to generate the response expansion coefficients c_{if}^{a} from equation 8 is as follows. An incoming angular current distribution over one mesh face *f* is given as a source for a single mesh. Vacuum boundary conditions are specified, and no current enters from the other five faces, such that for the sake of equation 9, $f'\neq f$:

$$\begin{aligned} J_{if}^{-} &= \Gamma^{a}\left(\vec{r},\hat{\Omega},E\right) \\ J_{if'}^{-} &= 0 \end{aligned} \tag{9}$$

A separate fixed source calculation is conducted for an incoming current source on each phase space expansion order on each unique face of each unique mesh in the core. A more detailed discussion of unique meshes is presented in section 3.2.1.

From each fixed-source calculation, the outgoing angular current J^+ is determined for all six faces *f'*. Using the orthogonality relationship, we solve equation 8 for $c_{if'}^{a'}$ given the calculated current exiting face *f'* as:

$$c_{if'}^{a'} = \iiint J_{if'}^{+}\left(\vec{r},\hat{\Omega},E\right)\Gamma^{a'}\left(\vec{r},\hat{\Omega},E\right)d\vec{r}\,d\hat{\Omega}\,dE \tag{10}$$

For a complete set of coefficients, equation 10 must be solved for all expansion orders *a'*. In order to implement this method, we return to the coordinate system of the problem. Therefore, the expansion coefficients for the angular current J^+ exiting face *f'* of mesh *i*, in group *g'*, with spatial and angular expansion orders *l'*, *m'*, and *n'* as a response to an incoming current on face *f* in group *g* having spatial and angular expansion orders *l*, *m*, and *n* are defined as equation 11:

$$c_{i,f',g',l',m',n'}^{ifglmn} = \int\int\int J_{if'}^{+}(u,\mu,\varphi,E)\widetilde{P}_{l'}^{[0,U]}(u)\widetilde{P}_{m'}^{[-1,1]}(\mu)\widetilde{P}_{n'}^{[0,\pi]}(\varphi)\delta_{g'}\,du\,d\mu\,d\varphi \tag{11}$$

It will be shown in chapter 4 that the higher the expansion orders *L*, *M*, and *N* at which the orthogonal series are truncated, the more accurate the results generated by the method will be.

3.1.1. Treatment of Hexagonal Geometry

Since in a hexagonal mesh, the spatial and angular variables defined by each mesh face will have different orientations, and since the planes defined by the mesh faces

themselves are not linearly independent, it is evident that a set of coordinate transformations must be introduced. The Cartesian coordinate system is used here for the sake of simplicity. Figure 1 depicts a typical hexagonal mesh in the Cartesian *x*-*y* plane.

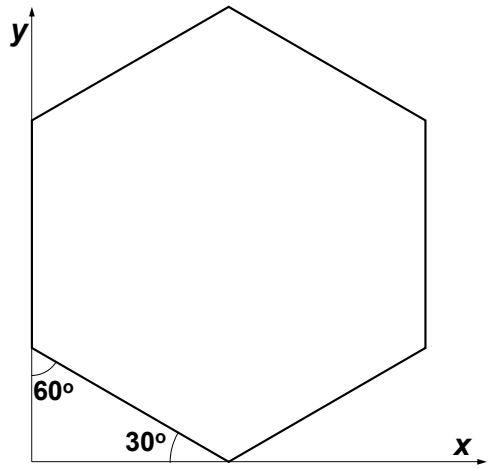

Figure 1. Mesh geometry in Cartesian coordinates

To illustrate the concept of a different coordinate system for each mesh face, consider figure 2. An example incoming source particle will be traveling from some position *u* in direction $\hat{\Omega}$ in three-dimensional space. Figure 2a shows a portion of the mesh from figure 1, but is focused specifically on the lower-left mesh face; the mesh boundary is represented by a dashed line. The projection of the direction vector $\hat{\Omega}$ onto the *x*-*y* plane is shown along with the angle φ, and the relation of the spatial coordinate *u* for this particular mesh face to the Cartesian *x*-*y* plane can be seen. The outward normal unit vector $\hat{n}$ from the mesh face is also shown. Figure 2b projects the direction vector onto

the plane defined by the Cartesian z axis and the outward normal of the mesh face $\hat{n}$. The angle θ is displayed, from which μ can be calculated.

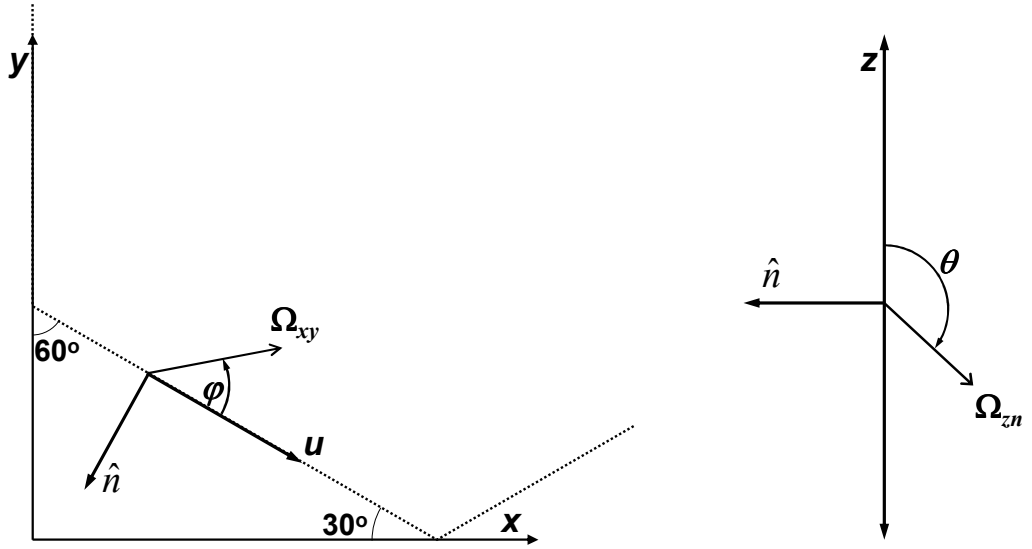

(a) projection onto x-y plane (b) projection onto z-n plane

Figure 2. Mesh coordinate systems for incoming source particles

The spatial coordinate u, defined along each mesh face, must be transformed into a coordinate in the Cartesian x-y plane. Similarly, the angles φ and μ defined from each mesh face must be transformed into some combination of the angular components Ω_x, Ω_y, and Ω_z. As an example, the Cartesian angular components for the face depicted are found using equation 12:

$$\Omega_x = \sqrt{1-\mu^2}\cos\left(\varphi - \frac{\pi}{6}\right)$$
$$\Omega_y = \sqrt{1-\mu^2}\sin\left(\varphi - \frac{\pi}{6}\right) \quad (12)$$
$$\Omega_z = \mu$$

A similar set of equations may be determined for each mesh face. In this way, the incoming angular current surface source defined by equation 9 is applied to the coarse mesh.

Neutrons will be transported through the mesh, with some being eventually absorbed within the mesh, and the rest escaping. An exiting neutron will be at some position along a mesh face and traveling at some angle defined in Cartesian geometry. A second coordinate transformation must be applied in order to solve equation 11, placing Cartesian coordinates back into the u, φ, and μ phase space variables defined by the mesh face. However, the coordinate system for particles leaving the mesh must be oriented so that the angular half-space over which the orthogonal expansion of the angular current is defined is that space outside of the mesh. This must be done so that the mesh boundary conditions given by equation 4 may be satisfied. Figure 3 shows an example mesh and its neighboring meshes; the mesh face coordinate systems for incoming neutrons are shown as dashed lines inside of the hexagonal meshes, while the mesh face coordinate systems for neutrons exiting the meshes are given as solid lines outside of the hexagonal meshes. The coordinate system used for particles exiting each mesh face is the same as the coordinate scheme for particles entering the neighboring mesh face.

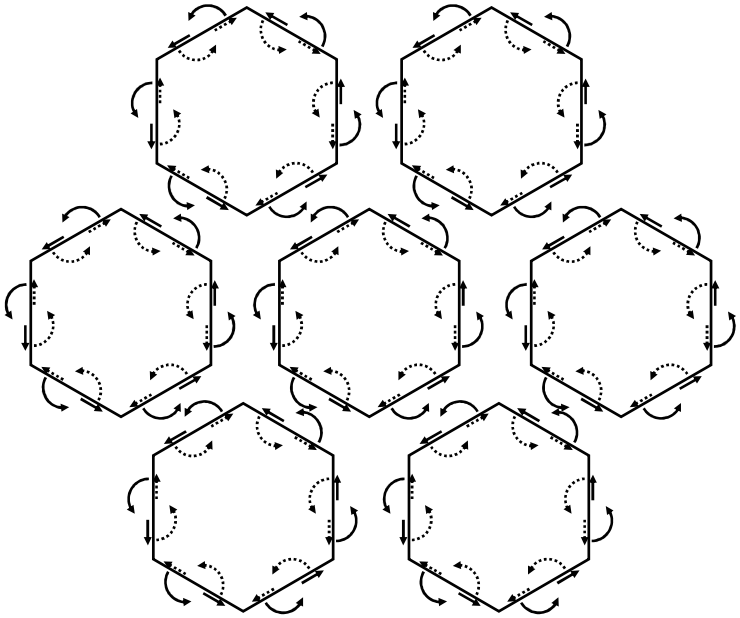

Figure 3. Interactions between meshes

3.2. Response Coefficient Library

Upon completion of the response function generation, the set of response coefficients is compiled into a data library. The library includes all coefficients for all desired combinations of the expansion orders present in the problem, so that for every unique mesh, the total number of response function coefficients to be stored for the angular current will be

$$K \times \left(F_{(u)} \cdot G \cdot (L+1) \cdot \Xi\right) \times \left(F \cdot G \cdot (L+1) \cdot \Xi\right) \tag{13}$$

for each of the $I_{(fuel)}$ meshes which are fuel blocks, and

$$\left(F_{(u)} \cdot G \cdot (L+1) \cdot \Xi\right) \times \left(F \cdot G \cdot (L+1) \cdot \Xi\right) \tag{14}$$

for each of the $I_{(nonfuel)}$ meshes which have no multiplying material present. Response coefficient calculations are conducted in fuel blocks at K different values of the core multiplication factor. Note that for two-dimensional hexagonal meshes, the parameter F is equal to six for all meshes, but the number of unique mesh faces $F_{(u)}$ may vary from mesh to mesh.

We introduce Ξ to represent the number of angular expansion terms. Forget and Rahnema (2006b) showed that generating response functions for $(M+1)\times(N+1)$ angular expansion orders would produce high-order cross terms which do not contribute to the solution. It is necessary to eliminate these in order to maintain a constant expansion order. Therefore, let Ξ represent the number of terms such that $m \le M$, $n \le N$, and $(m+n) \le \max(M, N)$.

The same library may be used for the analysis of any reactor core whose component blocks consist of some combination of the meshes in the library and whose core eigenvalue is within the range for which response coefficients have been calculated. The solutions for all problems presented in the following section will be calculated using the same response coefficient library.

3.2.1. Uniqueness of meshes

It has been noted that response expansion coefficients must be generated for the unique meshes present within the core. The uniqueness of a mesh depends solely on its geometry and material composition (i.e., its block design or type) and not its position within the core. Refer to the benchmark problem presented in section 4.3. In each core problem, there are 127 blocks present. However, there are only 8 unique meshes. 66 blocks are graphite reflectors composed of the same material; as they are identical except for their position in the core, response expansion coefficients need only be generated once for this particular mesh. Twelve blocks in the core are fuel blocks utilizing enrichment #3. These also are identical to each other, and as such, response expansion coefficients need only be generated once for this block design. As reactor cores generally consist of many blocks which are identical to each other in structure and material composition at core loading, having to generate response expansion coefficients for only the unique meshes rather than every individual block represents the key to this method's efficiency.

3.3. Deterministic Solution Construction

The final step in the method is a deterministic sweep which composes the solution to the problem. In some sequence, each mesh within the core is solved to determine the angular current response coefficient at each face. The effect of the sweeping order on the final solution will be analyzed in the following section; since the solutions of the fixed-source

transport problems within each mesh are independent of the solutions in neighboring meshes, the choice of sweeping order should not affect the accuracy of the solution. This will be shown in the following section of this paper. However, differing sweeping techniques may influence the speed of the convergence of the solution. Several sweeping strategies are here proposed and will be investigated: sweeping from the center mesh outward, from the outermost meshes inward, and through the core in rows of meshes. A diagram of the sweeping methods is included in figure 4.

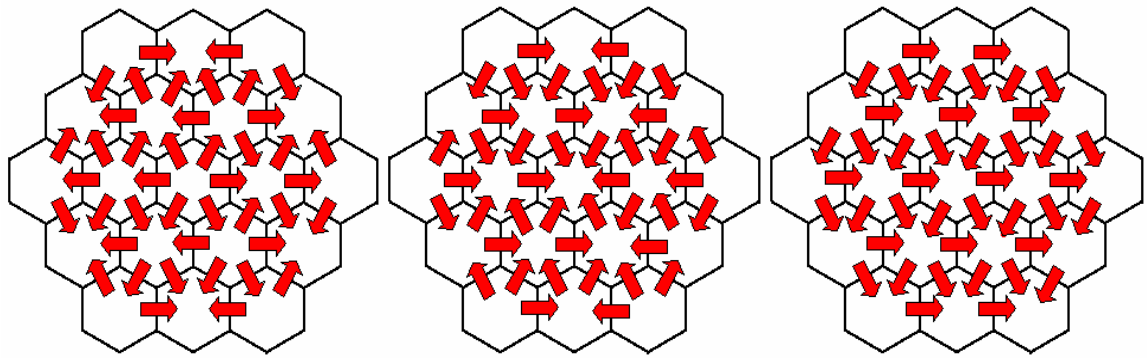

(a) In-Out (b) Out-In (c) Rows

Figure 4. Mesh sweeping schemes

Other deterministic solution algorithms were not considered in this paper, however, an investigation into the feasibility of other methods, such as the Chebyshev polynomial method described by Stamm'ler and Abbate (1983) should be conducted in the future.

4. RESULTS

In this chapter, the method is evaluated using a series of reactor eigenvalue problems. The problems chosen have been evaluated by Connolly, Rahnema, and Zhang previously (2011a, 2011b), and are here examined in greater detail. Benchmark problems describing a stylized high temperature gas-cooled reactor will be used as the bases for these calculations. The effect of the maximum expansion order of the angular current at mesh interfaces on the accuracy of the solution will be analyzed. An investigation is conducted to determine an optimal deterministic sweeping method.

4.1. Simple Test Problems

First, the performance of the new method will be evaluated with very simple problems. The problems illustrated here are not intended to portray realistic reactor designs, but merely to serve as test problems for methods development and error diagnostics. They are presented only to challenge the code's handling of sharp flux gradients, material boundaries, regions of high neutron leakage and absorption, and asymmetric systems. These test problems use the block structure and six-group cross section data from a benchmark problem (Zhang et al., 2009) based on the Japanese High Temperature Test Reactor (HTTR). Each core consists of three rings of prismatic blocks around a center block. The boundary of the system is corrugated as the method handles only full blocks. A boundary condition of no re-entrant particles is specified.

Three unique types of blocks are present in the core. The first is a fuel block, which is modeled as a hexagonal prismatic block of graphite with 33 fuel pins and 3 absorber pins. The fuel is treated as a pin consisting of a homogeneous mixture of graphite and a 4.3% enriched uranium oxide fuel compact, neglecting the heterogeneity due to the coated fuel particles in a graphite matrix. The absorber is a combination of boron carbide and carbon. In two of the test problems, control blocks are present which are modeled as graphite blocks with a single boron carbide control rod in the center. Reflector blocks are also present which consist solely of graphite. The three types of block geometry used are shown in figure 5.

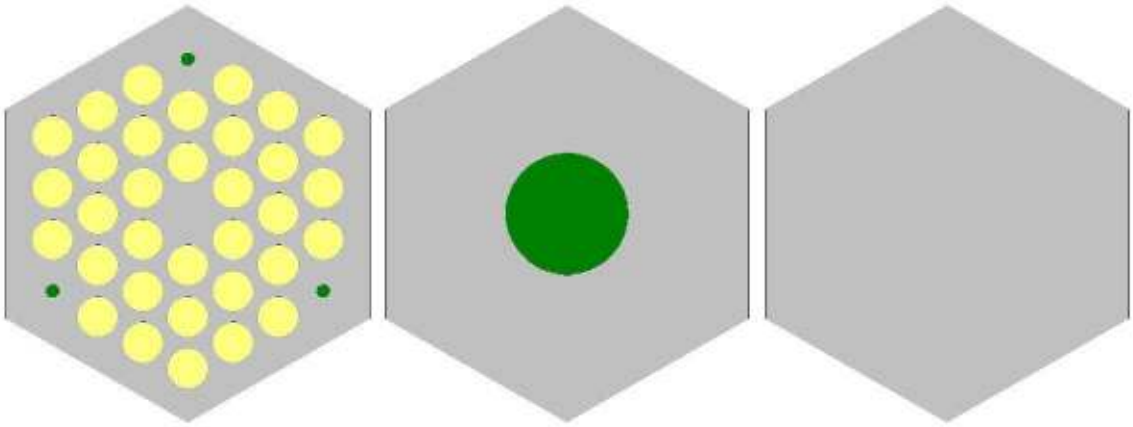

Figure 5. Fuel, control, and reflector blocks

As the first preliminary test, the simplest problem is presented. Let the first problem consist entirely of fuel blocks, as depicted in figure 6. This test is intended to challenge the performance of the method in a system with large flux gradients and a large amount of leakage.

MCNP5 (X-5 Monte Carlo Team, 2005) was used to acquire a reference solution. Five hundred million active particle histories were sampled for tallying after 62.5 million particle histories were skipped to converge the fission source. The system eigenvalue was found to be 0.84309 +/- 0.00003. The average statistical uncertainty in the pin fission densities was 0.067%, with the maximum pin fission density uncertainty at 0.19% for the six pins at the outermost corners of the core. All calculations presented in this paper were performed using 2 GHz processors with 16 GB of memory per eight-processor node. This calculation required 60.5 days of total computing time using 64 processors running in parallel.

As the first problem is quite simple, a second problem is now presented. The aim of the test is to introduce differing types of coarse meshes so as to challenge the method's performance in heterogeneous systems. This problem places a control block at the center of the reactor, and surrounds the core with reflectors. The core geometry is illustrated in figure 7. A reference solution was calculated in MCNP5 in which 500 million particle histories were sampled for tallying after skipping 62.5 million particle histories. The eigenvalue of the core was calculated to be 0.82156 +/- 0.00003. All pin fission densities were calculated to a statistical uncertainty of between 0.03% and 0.05%. This calculation required 63.7 days of computing time using 32 processors running in parallel.

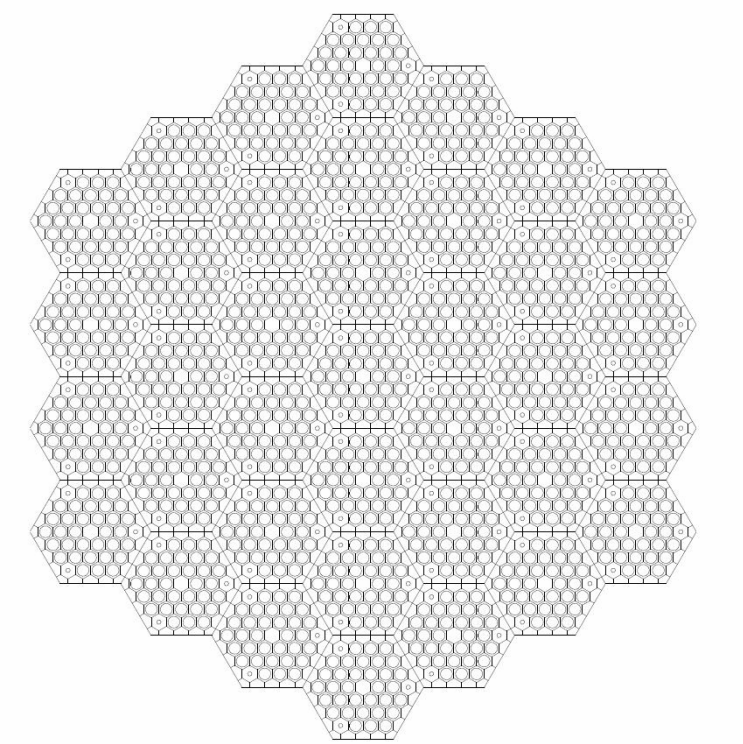

Figure 6. Test core #1

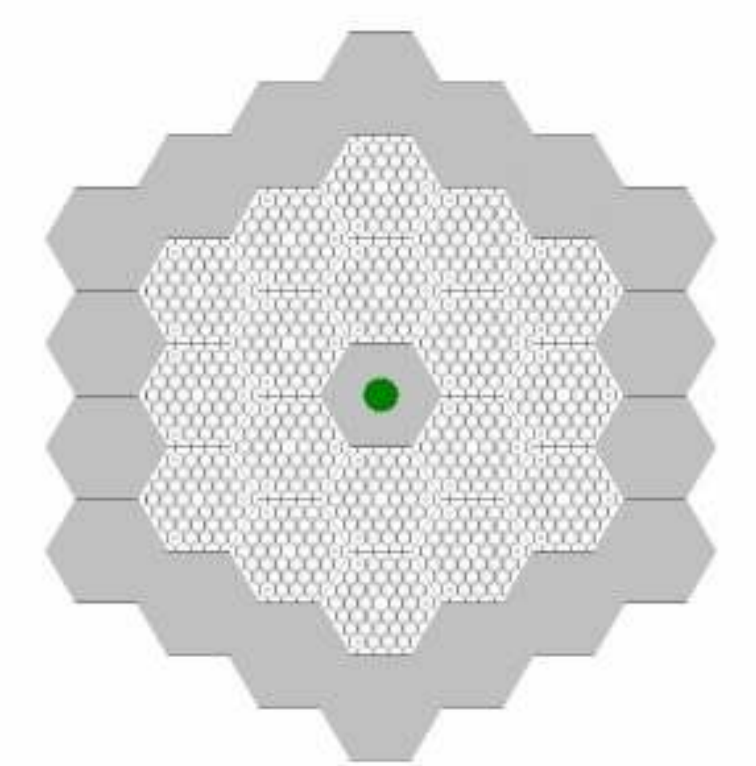

Figure 7. Test core #2

Now, in order to present a greater challenge to the capabilities of the method, a third and final problem is presented. This test case includes 27 fuel blocks, 4 reflector blocks, and 6 control blocks arranged as shown in figure 8. The power profile in the region surrounded by control blocks will be of special interest; low errors will demonstrate the method's accuracy even near absorbers. Furthermore, the core is asymmetric in order to illustrate that the method does not require symmetric problems to produce accurate solutions. The reference solution was calculated in MCNP as in the previous cases, skipping 62.5 million particle histories before running 500 million particle histories for tallying. This core eigenvalue was found to be 0.70840 +/- 0.00003. The average statistical uncertainty of the pin fission density tallies was 0.069%, with a maximum pin fission density uncertainty of 0.30%. All uncertainties over 0.2% were found in the fuel block on the outermost ring, in the corner, between the edge of the core and the control assemblies. This calculation took 54.2 days of computing time on 16 processors running in parallel.

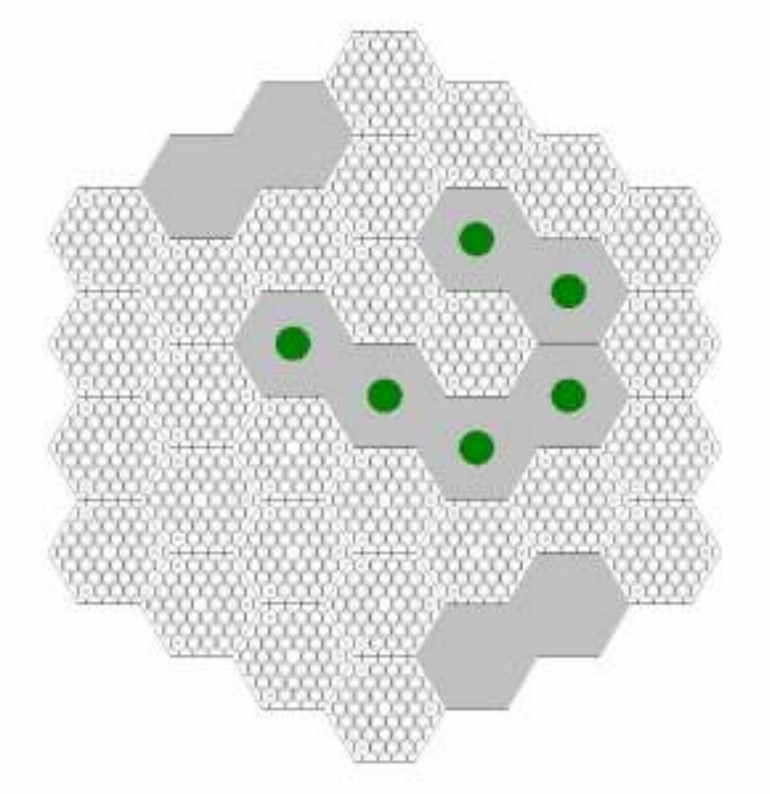

Figure 8. Test core #3

4.2. Simple Test Problem Results

In order to solve these problems, the response coefficient generator performed a total of 13,500 response function calculations, each requiring 10 million particle histories. A typical response function calculation for a fuel block required 12.5 minutes of computing time on a single processor; a typical calculation for a block without fuel required 2.75 minutes. The entire response function library was calculated in approximately 30 hours using 64 processors, roughly 80 days of total computing time. The collection of response functions was compiled in a database requiring 24.00 minutes on a single processor to complete. This database may be used for any reactor physics calculation with these assemblies and a core eigenvalue between 0.67 and 0.87.

Results are presented in Tables 1-3. Included in each table are the expansion orders for which the calculation was carried out in space, cosine of the polar angle, and azimuthal angle. That is, (L, M, N) in the first row of the table represents the maximum orders of l, m, and n from equation 7 which are used in the solution of the problem.

For the sake of the results presented in this paper, the definition used for the relative error in some quantity q will be as given in equation 14:

$$RE_q = \frac{q_{method} - q_{ref}}{q_{ref}} \tag{14}$$

The relative difference between the reference solution and the method solution for the eigenvalue is presented in the table for each test case and given in per cent mille. Since it would be impractical to present all pin fission density errors for full core problems, even for small cores such as these, the four rows which follow show several definitions of the average errors in the calculation of the pin fission densities. These include the average relative error between the method solution and the reference solution:

$$AVG = \frac{\sum_p \left| RE_p \right|}{P} \tag{15}$$

where the absolute relative error for each pin p is averaged over all P pins, the root mean squared error:

$$RMS = \sqrt{\frac{\sum_{p} RE_p^2}{P}} \tag{16}$$

the mean relative error:

$$MRE = \frac{\sum_{p} \left| RE_p \right| \cdot fd_p}{P \cdot fd_{avg}} \tag{17}$$

which weights the relative errors by the fission density of each pin fd_p and divides by the average pin fission density fd_{avg}, and the maximum relative error. Pin fission density results are given as per cent relative errors. Since many reactor analysis codes give block-averaged fission density rates, this data will also be included in the tables. The statistical uncertainty in the method's results will be presented in the table as well. The final value presented in each table is the computing time required to complete the calculation, given in seconds. Computation was conducted on a single processor.

All solutions utilized the same convergence criteria. Inner iterations on the current used a convergence ratio of 5×10^{-5}. As a safety check for inner iteration convergence, pin fission densities converged to 10^{-4}. Outer iterations on the eigenvalue used a convergence criterion of 5×10^{-5}. Cores were swept using the outward sweeping method illustrated in figure 4a, as this is demonstrated to be the fastest technique in section 4.5 of this paper.

Table 1. Test core #1 results

	(0,0,0)	(2,0,0)	(4,0,0)
k-eff (pcm)	-5247	1655	1780
$\sigma_{k\text{-}eff}$ (pcm)	6	6	6
Block AVG %	1.830	1.398	1.372
Block RMS %	2.333	1.759	1.727
Block MRE %	1.185	0.904	0.884
Block MAX %	4.342	3.511	3.383
Pin AVG %	3.272	1.867	1.752
Pin RMS %	6.225	2.494	2.294
Pin MRE %	1.899	1.016	1.032
Pin MAX %	33.002	6.216	5.880
AVG σ_{pin} (%)	0.058	0.069	0.071
MAX σ_{pin} (%)	0.133	0.184	0.186
Time (s)	14	9	10
	(0,2,2)	(2,2,2)	(4,2,2)
k-eff (pcm)	-5953	109	119
$\sigma_{k\text{-}eff}$ (pcm)	7	8	8
Block AVG %	2.984	0.182	0.180
Block RMS %	3.774	0.223	0.218
Block MRE %	1.925	0.140	0.138
Block MAX %	7.180	0.567	0.543
Pin AVG %	4.863	0.240	0.226
Pin RMS %	7.733	0.325	0.299
Pin MRE %	2.434	0.173	0.168
Pin MAX %	36.866	1.686	1.518
AVG σ_{pin} (%)	0.068	0.078	0.078
MAX σ_{pin} (%)	0.155	0.209	0.208
Time (s)	15	21	43
	(0,4,4)	(2,4,4)	(4,4,4)
k-eff (pcm)	-5996	50	60
$\sigma_{k\text{-}eff}$ (pcm)	7	8	8
Block AVG %	3.007	0.184	0.187
Block RMS %	3.803	0.218	0.220
Block MRE %	1.940	0.141	0.143
Block MAX %	7.229	0.501	0.487
Pin AVG %	4.909	0.230	0.226
Pin RMS %	7.808	0.299	0.288
Pin MRE %	2.454	0.171	0.173
Pin MAX %	37.183	1.158	1.350
AVG σ_{pin} (%)	0.069	0.080	0.080
MAX σ_{pin} (%)	0.158	0.212	0.213
Time (s)	18	43	102

The results for test core #1 are presented in Table 1. Core #1 includes 1221 fuel pins within the region. In the (2, 4, 4) case, 6 pins had relative errors of greater than 1.0%. All of these pins were found in the outermost ring of the core, where flux and power levels are lowest. The highest fission density of any of these pins was 0.22, and the other five were below 0.2.

It should be noted that the maximum statistical uncertainty of the pin fission density calculations was far greater than the average; these high uncertainties occurred at the outside of the core where individual pins had very low fission density values. This phenomenon will also appear in the third core.

The results for test core #2 are presented in Table 2. Again, the highest errors were in the pins at the core periphery, however, at the (2, 4, 4) and (4, 4, 4) order calculations the highest relative errors in the pin calculations were 0.6%. The lower errors in the pin fission density calculations in core #2 when compared with core #1 may be a result of the flatter flux profile in the second core. Core #1 is a bare reactor with a peaking factor of 2.347, and the pin with the lowest fission density in the first core has a value of only 0.059. In contrast, core #2 is surrounded by reflector blocks and has a control block in the center of the core. The fission densities of pins within the core range from 0.726 to 1.363.

Table 2. Test core #2 results

	(0,0,0)	(2,0,0)	(4,0,0)
k-eff (pcm)	-6221	1419	1539
$\sigma_{k\text{-}eff}$ (pcm)	7	7	7
Block AVG %	1.730	0.332	0.316
Block RMS %	1.832	0.385	0.367
Block MRE %	1.755	0.329	0.313
Block MAX %	2.350	0.756	0.700
Pin AVG %	1.918	0.723	0.683
Pin RMS %	2.165	0.903	0.812
Pin MRE %	1.904	0.705	0.667
Pin MAX %	4.601	2.660	1.907
AVG σ_{pin} (%)	0.048	0.050	0.052
MAX σ_{pin} (%)	0.051	0.054	0.055
Time (s)	16	12	12
	(0,2,2)	(2,2,2)	(4,2,2)
k-eff (pcm)	-6592	110	117
$\sigma_{k\text{-}eff}$ (pcm)	8	9	9
Block AVG %	1.205	0.167	0.166
Block RMS %	1.268	0.191	0.190
Block MRE %	1.226	0.161	0.160
Block MAX %	1.703	0.346	0.343
Pin AVG %	1.265	0.189	0.186
Pin RMS %	1.503	0.229	0.226
Pin MRE %	1.278	0.182	0.179
Pin MAX %	4.076	0.695	0.682
AVG σ_{pin} (%)	0.056	0.057	0.057
MAX σ_{pin} (%)	0.059	0.061	0.061
Time (s)	16	29	58
	(0,4,4)	(2,4,4)	(4,4,4)
k-eff (pcm)	-6626	57	64
$\sigma_{k\text{-}eff}$ (pcm)	8	9	9
Block AVG %	1.197	0.166	0.167
Block RMS %	1.259	0.190	0.191
Block MRE %	1.218	0.160	0.161
Block MAX %	1.692	0.341	0.343
Pin AVG %	1.252	0.188	0.188
Pin RMS %	1.491	0.227	0.228
Pin MRE %	1.267	0.181	0.181
Pin MAX %	4.044	0.589	0.597
AVG σ_{pin} (%)	0.057	0.058	0.058
MAX σ_{pin} (%)	0.059	0.062	0.062
Time (s)	19	63	139

Table 3. Test core #3 results

	(0,0,0)	(2,0,0)	(4,0,0)
k-eff (pcm)	> 5000	1649	1766
$\sigma_{k\text{-}eff}$ (pcm)	-	7	7
Block AVG %	-	3.021	3.034
Block RMS %	-	3.980	4.000
Block MRE %	-	2.144	2.158
Block MAX %	-	10.324	10.396
Pin AVG %	-	3.387	3.301
Pin RMS %	-	4.441	4.338
Pin MRE %	-	2.269	2.230
Pin MAX %	-	12.759	12.152
AVG σ_{pin} (%)	-	0.071	0.073
MAX σ_{pin} (%)	-	0.191	0.193
Time (s)	-	14	16
	(0,2,2)	(2,2,2)	(4,2,2)
k-eff (pcm)	> 5000	72	80
$\sigma_{k\text{-}eff}$ (pcm)	-	8	8
Block AVG %	-	0.153	0.158
Block RMS %	-	0.184	0.187
Block MRE %	-	0.128	0.133
Block MAX %	-	0.455	0.455
Pin AVG %	-	0.224	0.212
Pin RMS %	-	0.301	0.276
Pin MRE %	-	0.168	0.167
Pin MAX %	-	1.287	1.158
AVG σ_{pin} (%)	-	0.081	0.082
MAX σ_{pin} (%)	-	0.216	0.216
Time (s)	-	43	91
	(0,4,4)	(2,4,4)	(4,4,4)
k-eff (pcm)	> 5000	9	17
$\sigma_{k\text{-}eff}$ (pcm)	-	8	9
Block AVG %	-	0.127	0.131
Block RMS %	-	0.157	0.159
Block MRE %	-	0.094	0.097
Block MAX %	-	0.328	0.317
Pin AVG %	-	0.191	0.184
Pin RMS %	-	0.250	0.238
Pin MRE %	-	0.145	0.144
Pin MAX %	-	0.933	0.933
AVG σ_{pin} (%)	-	0.083	0.083
MAX σ_{pin} (%)	-	0.220	0.221
Time (s)	-	96	245

Calculations were attempted for the 0^{th} spatial order, but these calculations were not successfully completed. In all three attempts, the method began to converge on a multiplication factor outside of the range for which response expansion coefficients were generated. It can only be concluded that these calculations, had they been successfully completed, would have relative error in the eigenvalue calculation of over 5%, which would place them in line with calculations performed on the other two cores for the same expansion orders.

The results for the final test core are given in Table 3. The range of power levels within core #3 was the highest of the three test cores. The peaking factor was 2.451, and the lowest pin fission density in the core was only 0.022. Core #3 contains 891 fuel pins. Of those, only 9 pins were found to have relative fission density errors greater than 0.75% between the reference solution and the (2, 4, 4) calculation. The highest fission density found for one of those high-error pins was 0.43, and the eight other pins had fission density levels of at or below 0.25. Of special interest in core #3 was the fuel block surrounded on five sides by control blocks. For the (2, 4, 4) calculation, the average relative error in the pin fission densities in this block was 0.129%, with a maximum error of 0.337%. Due to some error cancellation, the average fission density calculated for the entire block was found to an error of 0.072%. These low errors show that the new method calculates accurate results even in regions near strong absorbers.

In all three core calculations, it is apparent that the expansion of both the spatial and angular variable above the zeroth order is essential for any meaningful results. Valid results are only produced once the spatial variable and the angular variables are expanded to at least the second order.

It can be seen in all three calculations that in these graphite-moderated systems, expanding the angular component of the flux from second order to fourth order leads to a reduction in the eigenvalue calculation by a factor of two, while expansion of the spatial component of the flux from second order to fourth order has no statistically significant effect on the eigenvalue calculation at all. In no case where the current was expanded in the angular variables to at least second order did the error in the eigenvalue change by greater than the convergence criteria plus σ or any of the errors in the pin fission density change by greater than the convergence criteria plus 2σ when the expansion order used was expanded from second order to fourth in the spatial variable. This is likely due to the fact that these graphite blocks have a higher neutron mean free path and a lower optical thickness. Variations in the flux due to pin-level heterogeneity will therefore be minor. It may be concluded that expansion of the spatial component of the current is unnecessary past a second-order expansion; if response function calculations were not conducted for expansion orders in space greater than 2, 40% fewer response function calculations would be performed.

The efficiency of the method can easily be seen. For each different core, MCNP reference solutions took many days of computing time to calculate. In contrast, the

method required a one-time computation of a response function library which took less computing time to complete than two full-core reference solutions. After that pre-computation was complete, the method was able to solve whole-core test problems exhibiting a range of eigenvalues and pin fission density levels in only a few minutes.

4.3. A realistic reactor problem

The method has proven its ability to accurately and efficiently solve several test problems, but it must also be evaluated against a more realistic reactor problem. This paper will adapt a different benchmark problem (Zhang et al., 2011), also based on the HTTR, in order to evaluate the accuracy of solutions calculated by the method. This problem has been chosen for its more realistic core design. The problem utilizes a cross section library with six energy groups; the same cross section set will be used for all response coefficient calculations. Eight unique coarse meshes are present within the core: four fuel blocks, two control blocks, and two reflector blocks. The block geometry to be used in the problems is presented in figure 9.

Two core configurations will be used as a starting point for the analysis of the accuracy of the hexagonal coarse mesh method. The first is the partially controlled core; the second is a core with all rods withdrawn. Figure 10 depicts the partially controlled core geometry. The uncontrolled core configuration has the same fuel layout but with all control rods withdrawn.

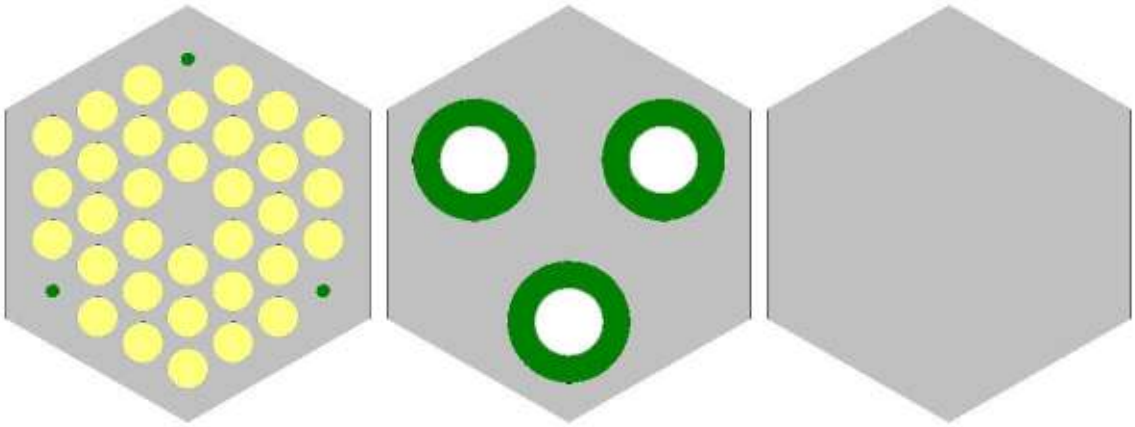

Figure 9. Block geometry. Depicted are representative fuel, control, and reflector blocks.

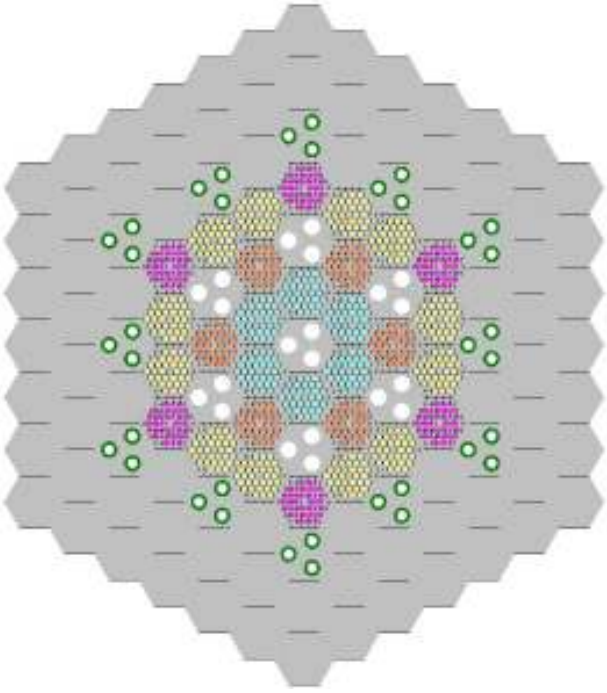

Figure 10. The partially-controlled core configuration.

Only the material and geometry specifications have been taken from the benchmark paper; new calculations are performed here for the sake of this analysis. A full core Monte Carlo calculation was conducted using MCNP5 in order to establish a reference

solution, including the eigenvalues and pin fission density distributions of both core configurations. A calculation conducted on the partially controlled core used 50,000 particle histories per cycle, and used 4,000 active cycles to compose the pin fission density profile and eigenvalue after 1,000 cycles were run to converge the fission source. The partially controlled core was found to have a multiplication factor of 1.01179 with an uncertainty of 0.00005. Pin fission densities were found for all 990 pins in the core; uncertainties in the fission density values ranged from 0.03-0.05%. The calculation was conducted over 7.5 hours on a 16-processor cluster. 2 GHz processors were used for all calculations in this paper.

The reference solution for the core with all rods withdrawn was found using 50,000 particles histories per cycle and 4,000 active cycles after the initial 1,000 cycles were used to converge the fission source. The reference value for the multiplication factor of the uncontrolled core was 1.13683 with an uncertainty of 0.00005. The uncertainty in the pin fission density calculations ranged from 0.03-0.04%. The calculation was conducted over 9.75 hours on a 16-processor cluster.

4.4. Response Expansion Coefficient Library

Response expansion coefficient calculations were performed for the eight unique meshes present in the reactor problem. For each calculation, the incoming current source given by equation 8 was presented using ten million incoming surface source neutrons sampled from the distribution defined by the product of the shifted Legendre polynomials.

All of the reactor calculations presented in the rest of this paper used the data from the same response expansion coefficient library. As indicated in the previous section, four unique multiplying meshes are present in the core, each with 33 fuel pins. Each fuel block has one-third rotational symmetry, and therefore two unique faces. Two control configurations are present in the core: a control block with rods inserted, and a control block with rods withdrawn. These also have one-third rotational symmetry. Finally, two reflector blocks are present, each with a different material specification. These blocks are one-sixth symmetric, and as such only have a single unique face. Using a six-group cross section library, and expanding the angular current to second order in space and fourth order in both angular variables, the parameters in equation 13 become G=6, L=2, and Ξ=15. For the two reflector blocks, F=6 and $F_{(u)}$=1; for the two control blocks, F=6 and $F_{(u)}$=2. For the four fuel blocks, F=6, $F_{(u)}$=2, P=33, and K=3. Response expansion calculations were performed for three values of the core eigenvalue: k=1.0, 1.1, and 1.2. These calculations required 14.5 hours on a 48 processor cluster.

To perform the control rod worth calculations for single rods in section 4.6, an additional unique mesh was introduced. Based on the control block, but with only one of the three rods inserted, the new block has six unique faces. Calculations required an additional 1.7 hours on 48 processors.

4.5. HTTR Problem Results and Sweeping Order Analysis

Solutions to the benchmark problems were calculated using the new method. Based on the expansion order analysis in section 4.2, a maximum expansion order of (2, 4, 4) is used for this problem.

It is desirable to determine an optimal scheme for conducting the deterministic sweep. In section 3.3, three different sweeping orders were proposed. They are evaluated below for the accuracy of the eigenvalue and pin fission density profile calculated, and for the speed of convergence. Table 4 shows the effects of the sweeping order on the partially controlled core; table 5 depicts results for the all-rods-out core configuration.

Table 4. Sweep Order Analysis of Partially Controlled Core

	Out -> In	In -> Out	Rows
k-eff (pcm)	-27	-33	-30
$\sigma_{k\text{-}eff}$ (pcm)	7	7	7
Block AVG %	0.030	0.026	0.033
Block RMS %	0.034	0.030	0.039
Block MRE %	0.031	0.027	0.033
Block MAX %	0.056	0.052	0.088
Pin AVG %	0.110	0.108	0.111
Pin RMS %	0.163	0.161	0.164
Pin MRE %	0.100	0.099	0.101
Pin MAX %	0.872	0.872	0.909
AVG σ_{pin} (%)	0.063	0.063	0.063
MAX σ_{pin} (%)	0.076	0.077	0.077
Time (s)	179	166	215

At most, six pins within the partially controlled core were calculated to have a relative error of over 0.8%. All of these pins were within the regions of the core at lowest power, the hottest of them having 0.53 times the fission density of the average fuel pin. As shown by the mean relative error figures, the relative errors were generally smaller in pins with higher fission density.

Table 5. Sweep Order Analysis of Uncontrolled Core

	Out -> In	In -> Out	Rows
k-eff (pcm)	-8	-11	-10
$\sigma_{k\text{-}eff}$ (pcm)	8	8	8
Block AVG %	0.038	0.038	0.045
Block RMS %	0.046	0.045	0.054
Block MRE %	0.038	0.038	0.045
Block MAX %	0.076	0.076	0.120
Pin AVG %	0.086	0.086	0.091
Pin RMS %	0.113	0.113	0.116
Pin MRE %	0.087	0.087	0.091
Pin MAX %	0.319	0.319	0.353
AVG σ_{pin} (%)	0.060	0.060	0.060
MAX σ_{pin} (%)	0.064	0.064	0.064
Time (s)	357	343	378

The high accuracy achieved by this new method is clear. In both cores, the average error in the pin fission density calculation was within the convergence criteria plus 2σ. The same is true of the eigenvalue calculation for the uncontrolled core. Although the calculated value of k_{eff} in the partially controlled core was not within the 95% confidence interval, the error was approximately 30 pcm regardless of the sweeping technique employed. The difference in solution time between the two trials was mostly a result of

the initial guess for k_{eff}; a better initial guess for the multiplication factor in the uncontrolled core would have sped up the convergence of the solution.

It can be seen that as expected, the differences in the relative errors resulting from different sweeping schemes are well within the confidence interval 2σ for the uncertainty of the solutions. Therefore, the in $\rightarrow$ out sweeping pattern is recommended as it produces results more quickly than the other methods.

4.6. Control rod worth analysis

The efficiency of the hexagonal coarse mesh method has been proven. An example is here presented to highlight both the benefits of using a pure transport method instead of a homogenized diffusion technique, and the computational speed of the method. These calculations will use the HTTR core and introduce a new block configuration for a control block with only one rod inserted. The reactivity worth of each control rod may be calculated using the all-rods-out configuration as a starting point. A change in reactivity ρ due to control rod insertion may be calculated as (Duderstadt and Hamilton, 1976):

$$\Delta\rho = \frac{k - k'}{k} \tag{16}$$

The multiplication factor of the core with all rods withdrawn shall be designated *k*. A full-core eigenvalue calculation will be conducted for the core with a single control rod inserted; eigenvalues will be determined for every unique configuration of the core with a

single rod in. The reactivity worth of each rod may then be calculated using equation 16, where *k'* will be the multiplication factor of the core with one rod in.

To again establish the capability of the method in solving full core problems, Table 6 presents the relative errors between the method solution and a reference solution calculated by MCNP5. This is a core with all rods out except one of the three center rods. The reference calculation used 100,000 particle histories per cycle, and ran 10,000 active cycles after skipping 6,000 inactive cycles. The calculated multiplication factor was 1.10268 +/- 0.00002, and the uncertainty in the fission density calculations was no greater than 0.04% for any of the 990 pins in the core. The calculation took 86.25 hours on 16 processors in parallel.

Table 6. Results for core with rod α inserted

k-eff (pcm)	0
$\sigma_{k\text{-eff}}$ (pcm)	8
Block AVG %	0.065
Block RMS %	0.074
Block MRE %	0.066
Block MAX %	0.131
Pin AVG %	0.105
Pin RMS %	0.136
Pin MRE %	0.105
Pin MAX %	0.859
AVG σ_{pin} (%)	0.060
MAX σ_{pin} (%)	0.071
Time (s)	227

Given the high accuracy of the results already presented, it would be unnecessary to calculate a reference solution for all eleven unique core configurations with a single rod inserted. The rod worth in per cent mille of reactivity is given in table 7 for core

calculations conducted at the expansion order (2, 4, 4). The uncertainty of the reactivity worth calculations for each rod is between 18 and 19 pcm in reactivity units. A one-sixth slice of the reactor is presented in figure 11 with each control rod labeled.

Table 7. Control rod worth

Rod	-ρ (pcm)
α	2993
β	2123
γ	1960
δ	1809
ε	989
ζ	905
η	737
θ	655
ι	608
κ	478
λ	377

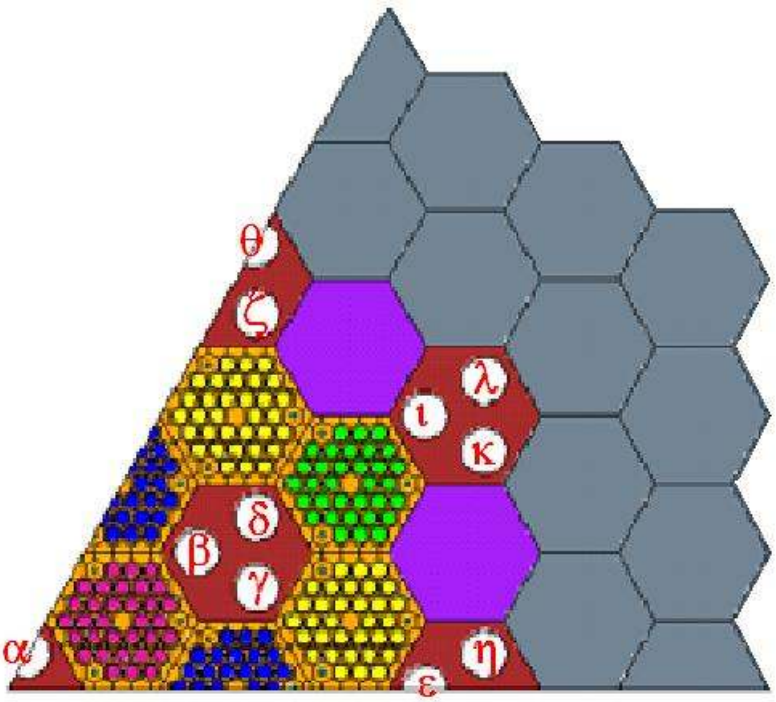

Figure 10. Control rod designations

This control rod analysis calculation is an example of a problem that diffusion-based and homogenization-based methods would be unable to solve. Because of its reliance on transport theory without approximation to the core design, this method yields accurate results quickly. This analysis required 12 eigenvalue calculations; one for the all-rods-out basis case, and one for each unique control rod placement. Only 61 minutes were required for the calculations. It has been shown that the hexagonal coarse mesh method can solve a variety of reactor core problems to a very high degree of accuracy in an order of minutes.

5. CONCLUSIONS

A new transport method has been developed for the whole core neutronics analysis of hexagonal geometry in two dimensions. The method is highly accurate and efficient. It uses a stochastic technique to generate a response expansion library and performs a deterministic sweep to compose the whole core solution. The method models the detailed heterogeneity of the core and produces detailed solutions nearly three orders of magnitude more quickly than full-core Monte Carlo calculations. It is highly accurate, determining core eigenvalues to an error on the order of 0.02%, and explicitly calculating the relative pin fission density of every individual fuel pin in the core to an average error of less than 0.1%. It has been shown that individual control rod worth can be calculated, highlighting the capability of the method.

An extension of the method to three-dimensional geometry is the next step in its development. In order to further establish the robust capability of this hexagonal coarse mesh method, it would be desirable to evaluate its performance in solving other reactor types, such as fast breeder reactor cores. It is anticipated that due to the high level of anisotropy in the flux within a fast reactor, it may be necessary to expand the angular current to a higher order, however, this is not expected to significantly challenge the method. However, due to the complex energy spectral effects within fast reactors, it may be necessary to use the continuous energy treatment instead of the multigroup treatment; because the method relies on Monte Carlo methods, it may be possible to due this in the future. The integration of some method for determining time-dependent behavior would

expand the capability of the method from solving only steady-state or eigenvalue problems to handling transient reactor calculations. Furthermore, a procedure for calculating burnup would allow COMET to perform core depletion (fuel cycle) calculations. Once extended to three dimensions, for practical reactor core calculations, the method should take thermal hydraulics into account. Such a versatile method would be a valuable tool for evaluating the safety and performance of a fleet of new reactors.

REFERENCES

Bell, G. I. and Glasstone, S., *Nuclear Reactor Theory*, Krieger, Malabar, Fla. (1970).

Chao, Y. A. and Shatilla, Y. A., "Conformal Mapping and Hexagonal Nodal Methods-II: Implementation in the ANC-H Code," *Nuclear Science and Engineering*, **121**, 210-25 (1995).

Cho, J. Y. and Kim, C. H., "Higher Order Polynomial Expansion Nodal Method for Hexagonal Core Neutronics Analysis," *Annals of Nuclear Energy*, **25**, 1021-31 (1998).

Cho, J.-Y., Kim, K.-S., Lee, C.-C., and Joo, H.-G., "Whole Core Transport Calculation for the VHTR Hexagonal Core," *13th International Conference on Emerging Nuclear Energy Systems*, Istanbul, Turkey, June 3-8 (2007).

Connolly, K. J., Rahnema, F., and Zhang, D., "COMET-Hex Solution to a 2-D Stylized High Temperature Test Reactor Benchmark," *Transactions of the American Nuclear Society* (2011) (accepted).

Connolly, K. J., Rahnema, F., and Zhang, D., "Extension of the COMET Method to 2-D Hexagonal Geometry," *International Conference on Mathematics and Computational Methods Applied to Nuclear Science and Engineering (M&C 2011)*, Rio de Janeiro, RJ, Brazil, May 8-12, 2011, on CD-ROM, Latin American Section (LAS) / American Nuclear Society (ANS) (2011).

Duderstadt, J. J. and Hamilton, L. J., *Nuclear Reactor Analysis*, John Wiley and Sons, New York (1976).

Forget, B. and Rahnema, F., "COMET Solution in a Highly Heterogeneous Boiling Water Reactor Benchmark Problem," *Transactions of the American Nuclear Society*, **95**, 709-12 (2006).

Forget, B. and Rahnema, F., "COMET Solutions to the 3-D C5G7 MOX Benchmark Problem," *Progress in Nuclear Energy*, **48**, 467-75 (2006).

Forget, B. and Rahnema, F., "COMET Solutions to Whole Core CANDU-6 Benchmark Problem," *PHYSOR-2006: Advances in Nuclear Analysis and Simulation*, American Nuclear Society's Topical Meeting on Reactor Physics, Vancouver, Canada, September 10-14 (2006).

Forget, B., Rahnema, F., and Mosher, S. W., "A Heterogeneous Coarse Mesh Solution for the 2-D NEA C5G7 MOX Benchmark Problem," *Progress in Nuclear Energy*, **45**, 233-54 (2004).

González-Pintor, S., Ginestar, D., and Verdú, G., "High Order Finite Element Method for the Lambda Modes Problem on Hexagonal Geometry," *Annals of Nuclear Energy*, **36**, 1450-62 (2009).

Idaho National Laboratory, "Summary for the Next Generation Nuclear Plant Project in Review," *INL/EXT-10-19142 Revision 1* (2010).

Lee, C. H., Joo, H. K., Yang, W. S., and Taiwo, T. A., "Implementation of Nodal Equivalence Parameters in DIF3D-VARIANT for Core Analysis of Prismatic Very High Temperature Reactor (VHTR)," Argonne National Laboratory, *ANL-GenIV-092* (2007).

Mosher, S. W. and Rahnema, F., "The Incident Flux Response Expansion Method for Heterogeneous Coarse Mesh Transport Problems," *Transport Theory and Statistical Physics*, **35**, 55-86 (2006).

Smith, M. A., Lewis, E. E., and Na, B.-C., "Benchmark on Deterministic Transport Calculations Without Spatial Homogenisation: A 2-D/3-D MOX Fuel Assembly Benchmark," Nuclear Energy Agency (2003).

Stamm'ler, R. J. J. and Abbate, M. J., *Methods of Steady-State Reactor Physics in Nuclear Design*, Academic Press, London (1983).

Thilagam, L., Jagannathan, V., Sunil sunny, C., and Subbaiah, K. V., "VVER-1000 MOX Core Computational Benchmark Analysis Using Indigenous Codes EXCEL, TRIHEX-FA, and HEXPIN," *Annals of Nuclear Energy*, **36**, 1502-15 (2009).

X-5 Monte Carlo Team, "MCNP—A General Monte Carlo N-Particle Transport Code, Version 5," Los Alamos National Laboratory (2005).

Zhang, Z., Rahnema, F., Pounders, J. M., Zhang, D., and Ougouag, A., "A Simplified 2D HTTR Benchmark Problem," *International Conference on Mathematics, Computational Methods & Reactor Physics (M&C 2009)*, Saratoga Springs, New York, May 3-7, 2009, on CD-ROM, American Nuclear Society, LaGrange Park, Ill. (2009).

Zhang, Z., Rahnema, F., Zhang, D., Pounders, J. M., and Ougouag, A., "Simplified Two and Three Dimensional HTTR Benchmark Problems," *Annals of Nuclear Energy*, **38**, 1172-85 (2011).